




## RESEARCH ARTICLE

# Genetic influences on neonatal cortical thickness and surface area

Shaili C. Jha<sup>1</sup> | Kai Xia<sup>1</sup> | James Eric Schmitt<sup>2</sup> | Mihye Ahn<sup>3</sup> | Jessica B. Girault<sup>1</sup>  |  
 Veronica A. Murphy<sup>1,4</sup> | Gang Li<sup>5</sup> | Li Wang<sup>5</sup>  | Dinggang Shen<sup>5</sup> | Fei Zou<sup>6</sup> |  
 Hongtu Zhu<sup>6,7</sup> | Martin Styner<sup>1,8</sup> | Rebecca C. Knickmeyer<sup>1</sup> | John H. Gilmore<sup>1</sup> 

<sup>1</sup>Department of Psychiatry, University of North Carolina, Chapel Hill, North Carolina

<sup>2</sup>Brain Behavior Laboratory, Departments of Radiology and Psychiatry, University of Pennsylvania, Philadelphia, Pennsylvania

<sup>3</sup>Department of Mathematics and Statistics, University of Nevada, Reno, Nevada

<sup>4</sup>Curriculum in Neuroscience, University of North Carolina, Chapel Hill, North Carolina

<sup>5</sup>Biomedical Research Imaging Center, University of North Carolina, Chapel Hill, North Carolina

<sup>6</sup>Department of Biostatistics, University of North Carolina, Chapel Hill, North Carolina

<sup>7</sup>Department of Biostatistics, The University of Texas MD Anderson Cancer Center, Houston, Texas

<sup>8</sup>Department of Computer Science, University of North Carolina, Chapel Hill, North Carolina

## Correspondence

John H. Gilmore,  
 Department of Psychiatry,  
 304 MacNider Hall, Campus Box #7160,  
 University of North Carolina,  
 Chapel Hill NC 27599-7160.  
 Email: john\_gilmore@med.unc.edu

## Funding information

National Science Foundation, Grant/Award Numbers: DMS-1407655, SES-1357666; National Institutes of Health, Grant/Award Numbers: R25GM055336, K01ES026840, T32 NS007431, MH109773, MH100217, MH107815, MH108914, HD079124, HD-003110, MH091645, MH086633, UL1 RR025747, MH083045, HD053000, MH070890, MH064065

## Abstract

Genetic and environmental influences on cortical thickness (CT) and surface area (SA) are thought to vary in a complex and dynamic way across the lifespan. It has been established that CT and SA are genetically distinct in older children, adolescents, and adults, and that heritability varies across cortical regions. Very little, however, is known about how genetic and environmental factors influence infant CT and SA. Using structural MRI, we performed the first assessment of genetic and environmental influences on normal variation of SA and CT in 360 twin neonates. We observed strong and significant additive genetic influences on total SA ( $a^2 = 0.78$ ) and small and nonsignificant genetic influences on average CT ( $a^2 = 0.29$ ). Moreover, we found significant genetic overlap (genetic correlation = 0.65) between these global cortical measures. Regionally, there were minimal genetic influences across the cortex for both CT and SA measures and no distinct patterns of genetic regionalization. Overall, outcomes from this study suggest a dynamic relationship between CT and SA during the neonatal period and provide novel insights into how genetic influences shape cortical structure during early development.

## KEYWORDS

brain development, gray matter, heritability, infant, MRI, twin

## 1 | INTRODUCTION

Individual variations in cortical thickness and surface area are associated with complex psychiatric and neurodevelopmental conditions, intellectual ability, and aging (Janssen et al., 2014; Long et al., 2012;

Shaw et al., 2006; Wolosin, Richardson, Hennessey, Denckla, & Mostofsky, 2009). Current evidence suggests CT and SA are independent phenotypes with strong, but distinct genetic underpinnings. Twin and family studies have revealed that overall total SA and average CT are highly heritable in adults, with genetic factors accounting for up to

89 and 81% of the total phenotypic variance respectively (Panizzon et al., 2009; Winkler et al., 2010). Regionally, heritability measures are found to vary significantly across the cortex, ranging from 17 to 76% for SA and from 6 to 73% for CT, after correcting for global measures (Winkler et al., 2010). These studies also reveal small and nonsignificant genetic correlations between CT and SA, suggesting that both phenotypes are driven by different sets of genetic factors. It has often been assumed that genetic independence in CT and SA reflects different cellular and neural processes occurring during fetal brain development. At present, however, the majority of heritability research has been performed in children, adolescents, and adults and there are no investigations that directly focus on genetic contributions to CT and SA during this foundational period of cortical development.

To better address the genetic underpinnings of CT and SA and their potential neurodevelopmental origins, it is critical to evaluate these cortical measures during prenatal and early postnatal periods. According to the radial unit hypothesis and the supragranular layer expansion hypothesis, surface area is primarily driven by the number of cortical columns generated during the early embryonic period and cortical thickness is determined by the number and size of cells within a column, packing density, as well as the number of neuronal processes, glial processes, and synapses arising primarily during the fetal and perinatal periods (Rakic, 1995, 2009). Additionally, CT and SA development are also regulated by outer radial glial cells which play a critical role in the radial and tangential expansion of the topmost layers of the cortex (Nowakowski, Pollen, Sandoval-Espinosa, & Kriegstein 2016). These developmental processes are associated with dynamic patterns of gene expression. Indeed, during the prenatal period, the majority of brain-expressed genes show strong temporal changes (Kang et al., 2011) and large regional differences in expression (Pletikos et al., 2014). During the early postnatal period, there is a shift in temporal and spatial gradients resulting in relatively stable levels of gene expression over time and minimal regional differences across the cortex. In adolescence, interareal differences in gene expression reemerge across the cortex (Kang et al., 2011; Pletikos et al., 2014; Silbereis, Pochareddy, Zhu, Li, & Sestan, 2016) and temporal gradients shift from being moderate to extremely rare by adulthood. Together, these findings suggest that genetic influences on cortical features are not set during the fetal period but are extremely dynamic across the lifespan; thus, heritability estimates for both CT and SA are likely to vary across different periods of development.

Moreover, twin studies of CT and SA during infancy may capture ongoing neurodevelopmental processes that are very different from those underlying heritability estimates in adults. During the neonatal period, the cortical surface expands 0.51% and the cortical mantle grows 0.09% per day (Jha et al., 2018). Dramatic growth of the cortex continues into the first 2 years with CT and SA reaching 97 and 64% of adult values, respectively (Lyll et al., 2015). In contrast, growth rates of CT and SA are relatively modest during childhood and adolescence (Gilmore, Knickmeyer, & Gao, 2018; Raznahan et al., 2011). Specifically, CT decreases linearly after the first 2 years and SA expands into late childhood but gradually declines thereafter. In addition to rapid CT and SA growth, our neuroimaging timepoint also captures the completion of primary gyrification and the beginning of primary myelination. Large-scale transformations in cortical

morphology that begin prenatally (Budday, Steinmann, & Kuhl, 2015; Kochunov et al., 2010) result in well-developed primary sulci and gyri by term birth (Hill et al., 2010). As cortical folds emerge, there is also rapid organization and myelination of white matter fiber bundles, peaking in the first year of life and leading to enhanced neuronal signaling (Dubois et al., 2014). Both primary gyrification and myelination contribute to early cortical development and likely influence the developmental trajectories of neonatal CT and SA.

Genes expressed at high levels during early fetal development are likely involved in neurogenesis, proliferation, and migration of neuronal cell types and genes expressed at high levels during late fetal and early postnatal development likely reflect neuronal and glial differentiation and the robust growth of dendrites and synapses (Stiles & Jernigan, 2010). These genes may be the primary drivers of rapid growth and variation in neonatal CT and SA. Genes driving CT and SA during later periods may be critical to processes of synaptic transmission and refinement, cell-cell signaling, and neurodegeneration (Pletikos et al., 2014). Interestingly, our recent genome-wide association study (GWAS) of neonatal neuroimaging phenotypes suggests that genetic determinants of neonatal brain volumes are highly distinct from those identified in imaging genetic studies in adolescents and adults (Xia et al., 2017). Thus, investigating genetic influences during this period will be crucial to our continued understanding of typical brain development and provide a deeper understanding of the heritability of rapidly growing cortical features like CT and SA.

In this article, we report findings from the first twin study of cortical thickness and surface area during infancy. We examine the genetic, shared environmental, and unique environmental contributions to individual differences in neonatal CT and SA using both global CT and SA as well as CT and SA measures in 78 cortical regions. We also assess genetic correlations among regions of interest (ROIs) for CT and SA measures to identify regions with shared genetic architecture. Based on the radial unit hypothesis, we predict that CT and SA will have independent genetic origins. Moreover, given the dynamic patterns of gene expression and interareal differences within the prenatal and early postnatal period, we hypothesize that heritability estimates will be highly distinct across the cortex. Outcomes from this study fill a critical gap in our understanding of how genetic influences shape cortical structure during early development and provide key insight for future imaging genetic studies of cortical structure.

## 2 | MATERIALS AND METHODS

### 2.1 | Subjects

This study included 234 dizygotic and 126 monozygotic twins between the ages of 9 and 92 postnatal days, drawn from the UNC Early Brain Development Study (Gilmore et al., 2010; Knickmeyer et al., 2008, 2016). Mothers with twin pregnancies were recruited during the second trimester of pregnancy from outpatient OB-GYN clinics in central North Carolina. Exclusion criteria included major medical illnesses in the mother or abnormal fetal ultrasounds. Zygosity was determined by polymerase chain reaction-short tandem repeat (PCR-STR) analysis of 14 loci on DNA extracted from buccal cells

**TABLE 1** Demographics for neonate twin sample

Continuous variables		Average	SD
Birth weight (g)		2,410.4	542.7
Gestational age at birth (days)		249.5	17.1
Postnatal age at MRI (days)		37.5	17.1
5 min Apgar		8.6	0.8
Maternal education (years)		15.0	3.3
Paternal education (years)		14.8	3.5
Maternal age (years)		30.4	5.6
Paternal age (years)		32.9	6.8
Categorical variables		N	%
Zygoty	Monozygotic	126	35%
	Dizygotic	234	65%
NICU stay >24 hr	No	236	66%
	Yes	124	34%
Sex	Male	203	56%
	Female	157	44%
Delivery method	Vaginal	98	27%
	C-section	262	73%
Household income	High	98	27%
	Mid	106	29%
	Low	136	38%
	Unknown	20	6%
Maternal ethnicity	Caucasian	274	76%
	African American	78	22%
	Asian	6	2%
	Native American	2	1%
Paternal ethnicity	Caucasian	266	74%
	African American	78	22%
	Asian	14	4%
	Native American	2	1%
Maternal psychiatric history	No	242	67%
	Yes	118	33%
Paternal psychiatric history	No	322	89%
	Yes	38	11%
Maternal smoking	No	340	94%
	Yes	20	6%
T2 sequence type	Type 1	118	33%
	Type 2	177	49%
	Type 3	11	3%
	Type 4	54	15%

(BRT Laboratories, Baltimore, MD). Detailed subject demographics can be viewed in Table 1. After complete description of the study to subjects' parent(s), written informed consent was obtained. Study protocols were approved by the Institutional Review Board of the UNC School of Medicine.

## 2.2 | Image acquisition

All MRI images were collected at UNC's Biomedical Research Imaging Center using a Siemens Allegra head-only 3 T scanner ( $N = 295$ ) or a Siemens TIM Trio 3 T scanner ( $N = 65$ ) (Siemens Medical System, Inc., Erlangen, Germany). Infants were scanned at  $37.5 \pm 17.1$  days post

birth on average. All neonate subjects were fitted with earplugs, secured into a vacuum-fixed immobilization device, and scanned during unседated natural sleep. Heart rate and oxygen saturation were monitored using a pulse oximeter. On the Allegra scanner, proton density and T2 weighted structural images were acquired using a turbo-spin echo sequence (TSE, TR = 6,200 ms, TE1 = 20 ms, TE2 = 119 ms, flip angle = 150°, spatial resolution = 1.25 mm × 1.25 mm × 1.95 mm, sequence name = Type1,  $N = 118$ ). For neonates who were deemed unlikely to sleep through the scan session, a "fast" turbo-spin echo sequence was collected using a decreased TR, a smaller image matrix, and fewer slices (TSE, TR range = 5,270–5,690 ms, TE1 range = 20–21 ms, TE2 range = 119–124 ms, flip angle = 150°, spatial resolution = 1.25 mm × 1.25 mm × 1.95 mm, sequence name = Type2,  $N = 177$ ). On the Trio, subjects were initially scanned using a TSE protocol (TR = 6,200 ms, TE1 = 17, TE2 = 116 ms, flip angle = 150°, spatial resolution = 1.25 mm × 1.25 mm × 1.95 mm, sequence name = Type3,  $N = 11$ ) while the rest were scanned using a 3DT2 SPACE protocol (TR = 3,200 ms, TE = 406, flip angle = 120°, spatial resolution = 1 mm × 1 mm × 1 mm, sequence name = Type4,  $N = 54$ ). Because sequence parameters could have a significant influence on cortical measures, we used T2 sequence (Type1–Type4) as a covariate in all of the analyses described in this study.

All T2 images were visually evaluated for motion artifacts. Two independent experts rated the motion of each image using a 4-point scale where 1 indicated no visible motion and 4 indicated significant motion artifacts. Average motion scores are summarized in Supporting Information Table S1. Images deemed unusable due to extreme levels of motion were excluded in this analysis.

## 2.3 | Image analysis

Cortical thickness and surface area measures were derived for all subjects using an image analysis pipeline previously described by Li et al. (2016). First, all T2-weighted images were preprocessed for tissue segmentation using a standard infant-specific pipeline (Li et al., 2013). This included skull stripping and manual editing of non-brain tissue, removal of the cerebellum and brain stem, corrections for intensity inhomogeneity, and finally, a rigid alignment of all the images into an average atlas space (Shi et al., 2011). Thereafter, an infant-specific path-driven coupled level sets method (described in Wang et al., 2014) was applied to segment gray matter (GM), white matter (WM), and cerebrospinal fluid (CSF). Non-cortical regions were masked, and tissues were divided into left and right hemispheres. A deformable surface method (Li et al., 2012, 2014) was then applied to the tissue segmentations to reconstruct the inner, middle, and outer cortical surfaces. The inner surface was defined as the boundary between gray and white matter and the outer surface was defined as the boundary between the gray matter and CSF. A third, middle cortical surface, was defined as the layer lying in the geometric center of the inner and outer surfaces of the cortex. The deformable surface method involved a topological correction of the WM to ensure spherical topology, a tessellation of the corrected WM to generate a triangular mesh, and the deformation of the inner mesh toward the reconstruction of each inner, middle, and outer surface.

All cortical surfaces for the left and right hemisphere were visually examined for accurate mapping. In order to generate a regional parcellation, all inner cortical surfaces were smoothed, inflated, and mapped to the unit sphere (Fischl, Sereno, & Dale, 1999). The cortical surfaces were parcellated into 78 regions of interest based on an infant-adapted 90 region parcellation atlas (Gilmore et al., 2012; Tzourio-Mazoyer et al., 2002). Twelve regions represent subcortical structures and were therefore not examined. CT was computed for each vertex as the average value of the minimum distance from the inner to the outer surfaces and the minimum distance from the outer to the inner surfaces. SA was computed based on the central cortical surface. The average CT and total SA were calculated for each ROI based on corresponding values at each vertex. Overall total SA was computed as the total over all regional SA values and overall average CT was computed by weighting regional CT values by the corresponding regional surface size.

## 2.4 | Statistical analysis

All statistical analyses were performed in R using OpenMx, a matrix-based structural equation modeling package (Boker et al., 2011; Neale & Cardon, 1992). Phenotypes of interest included: (a) overall average CT, (b) total SA, (c) regional CT in 78 ROIs, and (d) regional SA in 78 ROIs. Univariate analyses were performed using a classical ACE model, which allows for the decomposition of the observed phenotypic variance into variance explained by additive genetic ( $a^2$ ), shared environmental ( $c^2$ ), and unique environmental ( $e^2$ ) components. Maximum likelihood was used to generate estimates of model parameters and to perform hypothesis testing via the likelihood ratio test (Schmitt et al., 2008). The significance of genetic and shared environmental effects was assessed by removing a parameter of interest and comparing the resulting change in the maximum log-likelihood of the submodel against the original model, or the likelihood ratio test (LRT). The LRT asymptotically follows a  $\chi^2$  distribution, with degrees of freedom equal to the difference in the number of free parameters (Neale & Cardon, 1992) under the null hypothesis. For hypothesis tests on variance components,  $p$ -values were adjusted to account for boundary constraints of the ACE model (Dominicus, Skrondal, Gjessing, Pedersen, & Palmgren, 2006).

Bivariate Cholesky decomposition models were used to identify common genetic and environmental determinants between global CT, SA, and ICV, between regional CT measures, and between regional SA measures. The Cholesky decomposition model allows for the covariance between two phenotypes to be segregated into covariance resulting from either genetic or environmental sources (Neale & Cardon, 1992). Genetic and environmental covariance matrices were standardized to calculate the genetic and environmental correlations between phenotypes. The genetic correlation represents an estimate of the shared additive genetic effects between two phenotypes.

In both univariate and bivariate analyses, models for regional and total average CT were adjusted for birth weight, gestational age at birth, age at MRI, sex, paternal education, and maternal ethnicity. Models for regional SA were adjusted for birth weight, age at MRI and sex. The model for total SA was adjusted for birth weight,

gestational age at birth, age at MRI, and sex. Covariates were chosen based on output from variable selection and linear mixed effects model results for CT and SA in a large sample of neonates (Jha et al., 2018). To account for overall brain size, total surface area was fixed for all regional surface area models and the cubed root of intracranial volume (a sum of gray matter, white matter, and cerebrospinal fluid) was fixed in the models for average and regional cortical thickness. As a sensitivity analysis, univariate variance decomposition and bivariate Cholesky decomposition models were also run without adjusting for overall brain size. A sensitivity analysis was also performed controlling for traditional variables used in adult studies: scan parameters, brain size, age at MRI, and sex. In order to evaluate for potential confounds due to heteroscedasticity in ROI variance (e.g., changes in heritability of cortical thickness with age or sex), we repeated our ACE models with additional parameters allowing for variance components to vary with our covariates (Purcell, 2002; Wallace et al., 2006). For all regional analyses of CT and SA, adjustments for multiple comparisons were made using false discovery rate (Benjamini & Hochberg, 2000). FDR less than 0.05 was considered significant for each region of interest.

## 3 | RESULTS

Cross-twin correlations for CT and SA are presented in Table 2. In general, MZ twin pairs had increased correlations when compared with DZ twin pairs.

### 3.1 | Global CT and SA

Parameter estimates and tests of significance for global CT and SA are presented in Table 3. Overall, shared environmental influences had small and nonsignificant impacts on global CT and SA variation. Total SA was highly heritable, with genetic influences accounting for a large portion of the observed variance ( $a^2 = 0.78$ ,  $p < .001$ ). For average CT, genetic influences accounted for a small ( $a^2 = 0.29$ ,  $p > .05$ ) and nonsignificant proportion of the phenotypic variance. The observed genetic correlation between average CT and total SA was strong and significant ( $r_G = 0.65$ ,  $p < .05$ , see Table 4). To understand the impact of overall brain size on CT and SA, we also examined the heritability of intracranial volume (ICV). Genetic influences on ICV accounted for a significantly large amount of the total phenotypic variance ( $a^2 = 0.60$ ,  $p < .001$ ). Significantly high genetic correlations were found between ICV and total SA ( $r_G = 0.98$ ,  $p < .001$ ) and between ICV and overall average CT ( $r_G = 0.64$ ,  $p < .05$ ). Phenotypic (rP), common environmental (rC), and unique environmental (rE) correlations for global measures can be found in Table 4.

### 3.2 | Regional CT and SA

Parameter estimates for regional CT and SA are presented in Figure 1 and provided with tests of significance in Tables 5 and 6. The  $p$ -value and  $q$ -value thresholds were set at  $p < .05$ . For CT, regional heritability estimates ranged from  $<0.01$  to 0.52 with significant genetic effects in 9 of the 78 regions. After correcting for multiple

**TABLE 2** Co-twin correlations for MZ and DZ pairs

Region of interest	Cortical thickness		Surface area	
	MZ	DZ	MZ	DZ
Total SA	-	-	0.92	0.75
Average thickness	0.80	0.66	-	-
Precentral_L	0.56	0.52	0.76	0.54
Precentral_R	0.63	0.49	0.82	0.56
Frontal_Sup_L	0.69	0.55	0.53	0.59
Frontal_Sup_R	0.71	0.63	0.76	0.64
Frontal_Sup_Orb_L	0.53	0.49	0.62	0.44
Frontal_Sup_Orb_R	0.59	0.51	0.65	0.61
Frontal_Mid_L	0.63	0.55	0.82	0.57
Frontal_Mid_R	0.58	0.58	0.83	0.65
Frontal_Mid_Orb_L	0.20	0.28	0.71	0.42
Frontal_Mid_Orb_R	0.53	0.31	0.78	0.55
Frontal_Inf_Oper_L	0.47	0.28	0.59	0.49
Frontal_Inf_Oper_R	0.43	0.18	0.64	0.40
Frontal_Inf_Tri_L	0.61	0.37	0.62	0.41
Frontal_Inf_Tri_R	0.37	0.30	0.72	0.39
Frontal_Inf_Orb_L	0.49	0.49	0.87	0.54
Frontal_Inf_Orb_R	0.57	0.38	0.84	0.56
Rolandic_Oper_L	0.51	0.38	0.79	0.48
Rolandic_Oper_R	0.38	0.28	0.75	0.55
Supp_Motor_Area_L	0.61	0.37	0.69	0.58
Supp_Motor_Area_R	0.50	0.44	0.78	0.60
Olfactory_L	0.22	0.22	0.55	0.24
Olfactory_R	0.29	0.30	0.67	0.24
Frontal_Sup_Medial_L	0.55	0.39	0.61	0.51
Frontal_Sup_Medial_R	0.51	0.33	0.78	0.61
Frontal_Med_Orb_L	0.25	-0.01	0.40	0.33
Frontal_Med_Orb_R	0.47	0.21	0.76	0.56
Rectus_L	0.52	0.14	0.62	0.34
Rectus_R	0.43	0.14	0.70	0.52
Insula_L	0.72	0.38	0.82	0.60
Insula_R	0.72	0.43	0.84	0.63
Cingulum_Ant_L	0.36	0.29	0.68	0.35
Cingulum_Ant_R	0.18	0.38	0.84	0.63
Cingulum_Mid_L	0.56	0.39	0.71	0.46
Cingulum_Mid_R	0.50	0.46	0.89	0.61
Cingulum_Post_L	0.32	0.04	0.70	0.30
Cingulum_Post_R	0.15	0.24	0.59	0.41
ParaHippocampal_L	0.60	0.25	0.52	0.17
ParaHippocampal_R	0.50	0.05	0.74	0.39
Calcarine_L	0.35	0.44	0.68	0.44
Calcarine_R	0.37	0.31	0.68	0.31
Cuneus_L	0.26	0.17	0.58	0.36
Cuneus_R	0.08	0.23	0.67	0.32
Lingual_L	0.30	0.41	0.74	0.56
Lingual_R	0.31	0.46	0.82	0.68
Occipital_Sup_L	0.19	0.39	0.66	0.42
Occipital_Sup_R	0.18	0.21	0.62	0.45
Occipital_Mid_L	0.50	0.49	0.74	0.58
Occipital_Mid_R	0.34	0.24	0.67	0.58

(Continues)

TABLE 2 (Continued)

Region of interest	Cortical thickness		Surface area	
	MZ	DZ	MZ	DZ
Occipital_Inf_L	0.45	0.17	0.55	0.47
Occipital_Inf_R	0.55	0.33	0.59	0.48
Fusiform_L	0.53	0.32	0.59	0.58
Fusiform_R	0.53	0.41	0.69	0.50
Postcentral_L	0.65	0.42	0.70	0.47
Postcentral_R	0.64	0.44	0.80	0.62
Parietal_Sup_L	0.52	0.47	0.48	0.40
Parietal_Sup_R	0.28	0.37	0.86	0.68
Parietal_Inf_L	0.37	0.30	0.66	0.51
Parietal_Inf_R	0.43	0.30	0.69	0.57
SupraMarginal_L	0.33	0.15	0.55	0.35
SupraMarginal_R	0.32	0.33	0.79	0.56
Angular_L	0.17	0.02	0.60	0.32
Angular_R	0.50	0.36	0.69	0.54
Precuneus_L	0.49	0.20	0.86	0.52
Precuneus_R	0.30	0.22	0.88	0.73
Paracentral_Lobule_L	0.56	0.25	0.60	0.33
Paracentral_Lobule_R	0.36	0.12	0.68	0.47
Heschl_L	0.38	0.13	0.60	0.07
Heschl_R	0.58	0.30	0.60	0.31
Temporal_Sup_L	0.45	0.23	0.80	0.53
Temporal_Sup_R	0.55	0.17	0.84	0.67
Temporal_Pole_Sup_L	0.43	0.17	0.80	0.57
Temporal_Pole_Sup_R	0.25	0.26	0.75	0.65
Temporal_Mid_L	0.46	0.29	0.76	0.58
Temporal_Mid_R	0.59	0.43	0.86	0.61
Temporal_Pole_Mid_L	0.36	0.08	0.73	0.36
Temporal_Pole_Mid_R	0.51	0.29	0.75	0.51
Temporal_Inf_L	0.67	0.25	0.73	0.45
Temporal_Inf_R	0.55	0.37	0.87	0.63

comparisons, one region remained significant (right insula, see Table 5). Genetic correlations of regional CT ranged from  $-1.00$  to  $1.00$  (Figure 2a), with 83 significant relationships. No significant correlations were found across regions after correcting for multiple comparisons. Heritability estimates for regional SA ranged from  $<0.01$  to  $0.76$  with significant genetic influences in 28 of the 78 regions. Of these, genetic influences remained significant in 7 regions after a correction for multiple comparisons (left inferior orbitofrontal cortex, left and right insula, left and right precuneus, right supramarginal gyrus, and right inferior temporal gyrus, see Table 6). Genetic correlations of regional SA also ranged from  $-1.00$  to  $1.00$  (Figure 2b) with 131 significant relationships. No significant correlations remained after FDR correction. Overall, shared environmental influences had small and nonsignificant impacts on variation in regional CT or SA.

Regional genetic correlations between CT and SA were calculated for all 78 ROIs (see Figure 3). Results ranged from  $-1.00$  to  $1.00$ , with 65 of the 78 ROIs showing positive correlations and 7 showing significant genetic correlations. After correcting for multiple comparisons, significant genetic relationships remained between CT and SA in the right postcentral gyrus ( $r_G = 1.00$ ) and left precuneus ( $r_G = 0.67$ ).

### 3.3 | Secondary analyses

In a secondary analysis, genetic influences on CT and SA were examined without adjusting for overall brain size (Figure 4). For regional CT, heritability estimates ranged from  $<0.01$  to  $0.56$  and were significant in 13 of the 78 ROIs. Two significant genetic influences remained after FDR correction (left and right insula, see Supporting Information Table S2). For regional SA, heritability estimates ranged from  $<0.01$  to  $0.83$  and were significant in 65 of the 78 ROIs. After correction for

TABLE 3 Univariate ACE model maximum likelihood parameter estimates and  $p$ -values for global measures

Region of interest	Variance components			Variance component hypothesis test ( $p$ -values)		
	$a^2$	$c^2$	$e^2$	A	C	A and C
Total SA	0.78	0.11	0.10	<b>&lt;.001</b>	.343	<b>&lt;.001</b>
Average CT	0.29	0.18	0.53	.439	.500	<b>&lt;.001</b>
ICV	0.60	0.23	0.17	<b>&lt;.001</b>	.124	<b>&lt;.001</b>

A = test of genetic effects; C = test of shared environmental effects; A and C = test of familial effects (genetic + environmental). Bold/italicized text indicates  $p$ -values below 0.05.



**TABLE 4** Bivariate ACE model maximum likelihood parameter estimates and *p*-values for global measures

Regions of interest		Correlation coefficient				ROI-ROI covariance hypothesis test ( <i>p</i> -values)				
1	2	rP	rG	rC	rE	A	C	E	A and C	A, C, and E
Total SA	Average CT	0.32	0.65	0.30	-0.20	.005	.463	<.001	<.001	<.001
Total SA	ICV	0.86	0.98	0.82	0.50	<.001	.335	.002	<.001	<.001
Average CT	ICV	0.58	0.64	0.79	0.39	.025	.677	.132	<.001	<.001

A = test of genetic covariance; C = test of shared environmental covariance; A and C = test of familial covariance (genetic + environmental); A, C, and E = test of all and any covariance. Bold/italicized text indicates *p*-values below 0.05.

multiple comparisons, estimates were significant in 64 of the 78 ROIs (Supporting Information Table S3). Genetic correlations for regional CT and regional SA ranged from -1.00 to 1.00 (Supporting Information Figures S1 and S2). For regional CT, 196 significant correlations were found and one (between the left and right insula,  $r_G = 0.95$ ) remained after FDR correction. For regional SA, there were 2,240 significant correlations across various regions of interest and 2,106 survived FDR correction. Shared environmental influences remained small and nonsignificant for both regional CT and SA.

Most twin studies of CT and SA are performed during childhood, adolescence, and adulthood, and often do not have access to detailed prenatal demographics that may serve as important covariates. Therefore, to be consistent with analyses performed in the literature, we performed an additional sensitivity analysis controlling for variables most often used as covariates at later ages: brain size, age, sex, and scanner parameters (Figure 5). We observed significant genetic and common environmental influences on total SA (0.30 and 0.62, respectively) and on ICV (0.38 and 0.52, respectively). There were no significant genetic or common environmental influences on CT (Supporting Information Table S4). Genetic correlations were 0.65 between CT and SA, 0.97 between total SA and ICV, and 0.69 between average CT and ICV (Supporting Information Table S5). For regional CT,

heritability estimates ranged from <0.01 to 0.57 and were significant in 11 of the 78 ROIs (Supporting Information Table S6). One significant genetic influence remained after FDR correction (right insula). For regional SA, heritability estimates ranged from <0.01 to 0.73 and were significant in 28 of the 78 ROIs (Supporting Information Table S7). After correction for multiple comparisons, estimates were significant in the same 7 ROIs found in our primary analysis (left inferior orbitofrontal cortex, left and right insula, left and right precuneus, right supramarginal gyrus, and right inferior temporal gyrus). Genetic correlations for regional CT and regional SA ranged from -1.00 to 1.00 and one genetic relationship was significant for CT after FDR correction (left and right insula,  $r_G = 0.92$ , Supporting Information Figures S3 and S4).

Additive genetic x covariate interactions were not statistically significant for the vast majority of ROI x covariate combinations and did not substantially alter our primary results.

## 4 | DISCUSSION

Utilizing a sample of 360 twin neonates, we performed the first quantitative genetic study of infant CT and SA. Our results revealed strong

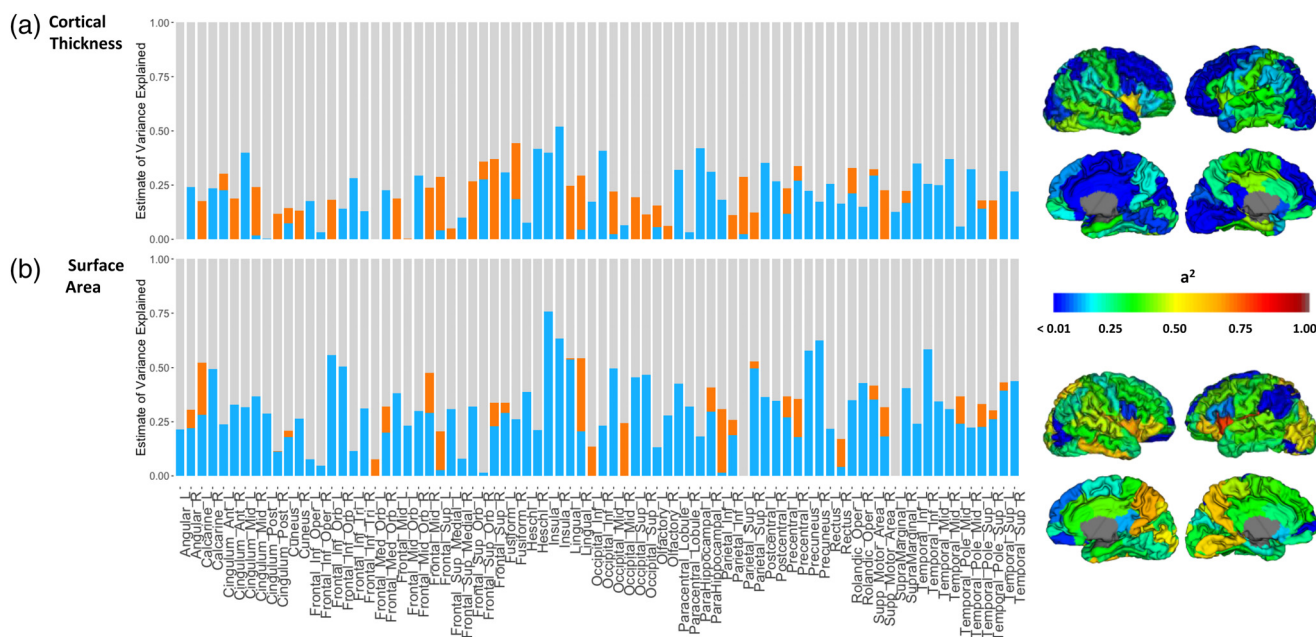


**FIGURE 1** Genetic, common environmental, and unique environmental influences on neonatal (a) cortical thickness and (b) surface area for 78 cortical regions. Genetic influences are displayed in blue, common environmental influences are displayed in orange, and unique environmental influences are displayed in gray. Genetic influences are also projected onto the cortical surface. Subcortical regions are in gray and were not analyzed

**TABLE 5** Univariate ACE model maximum likelihood parameter estimates and *p*-values for regional CT measures

Region of interest	Variance components			Hypothesis test <i>p</i> -values			Hypothesis test <i>Q</i> -values		
	$a^2$	$c^2$	$e^2$	A	C	A and C	A	C	A and C
Precentral_L	0.12	0.12	0.77	.349	.290	<b>.014</b>	.500	.500	<b>.034</b>
Precentral_R	0.27	0.07	0.66	.183	.367	<b>.002</b>	.451	.500	<b>.007</b>
Frontal_Sup_L	0.04	0.24	0.71	.439	.119	<b>&lt;.001</b>	.500	.500	<b>.003</b>
Frontal_Sup_R	<b>&lt;0.01</b>	0.37	0.63	.500	<b>.018</b>	<b>&lt;.001</b>	.500	.500	<b>&lt;.001</b>
Frontal_Sup_Orb_L	<b>&lt;0.01</b>	0.27	0.73	.500	.070	<b>.001</b>	.500	.500	<b>.004</b>
Frontal_Sup_Orb_R	0.28	0.08	0.64	.153	.350	<b>&lt;.001</b>	.451	.500	<b>.003</b>
Frontal_Mid_L	<b>&lt;0.01</b>	0.19	0.81	.500	.093	<b>.020</b>	.500	.500	<b>.041</b>
Frontal_Mid_R	<b>&lt;0.01</b>	0.24	0.76	.500	<b>.027</b>	<b>.003</b>	.500	.500	<b>.011</b>
Frontal_Mid_Orb_L	<b>&lt;0.01</b>	<b>&lt;0.01</b>	1.00	.500	.488	.500	.500	.500	.500
Frontal_Mid_Orb_R	0.29	<b>&lt;0.01</b>	0.71	.126	.500	<b>.017</b>	.439	.500	<b>.037</b>
Frontal_Inf_Oper_L	0.18	<b>&lt;0.01</b>	0.82	.182	.500	.101	.451	.500	.147
Frontal_Inf_Oper_R	0.03	<b>&lt;0.01</b>	0.97	.390	.500	.481	.500	.500	.500
Frontal_Inf_Tri_L	0.28	<b>&lt;0.01</b>	0.72	.055	.500	<b>.005</b>	.363	.500	<b>.014</b>
Frontal_Inf_Tri_R	0.13	<b>&lt;0.01</b>	0.87	.259	.500	.209	.499	.500	.254
Frontal_Inf_Orb_L	<b>&lt;0.01</b>	0.18	0.82	.500	.130	<b>.025</b>	.500	.500	<b>.049</b>
Frontal_Inf_Orb_R	0.14	<b>&lt;0.01</b>	0.86	.267	.500	.228	.500	.500	.273
Rolandic_Oper_L	0.21	0.12	0.67	.218	.288	<b>&lt;.001</b>	.463	.500	<b>.003</b>
Rolandic_Oper_R	0.15	<b>&lt;0.01</b>	0.85	.210	.500	.174	.463	.500	.218
Supp_Motor_Area_L	0.29	0.03	0.68	.174	.440	<b>.005</b>	.451	.500	<b>.014</b>
Supp_Motor_Area_R	<b>&lt;0.01</b>	0.23	0.77	.500	.090	<b>.005</b>	.500	.500	<b>.014</b>
Olfactory_L	0.06	0.10	0.84	.426	.329	.092	.500	.500	.140
Olfactory_R	<b>&lt;0.01</b>	0.06	0.94	.500	.287	.355	.500	.500	.407
Frontal_Sup_Medial_L	<b>&lt;0.01</b>	0.05	0.95	.500	.307	.395	.500	.500	.439
Frontal_Sup_Medial_R	0.10	<b>&lt;0.01</b>	0.90	.166	.500	.312	.451	.500	.363
Frontal_Med_Orb_L	<b>&lt;0.01</b>	<b>&lt;0.01</b>	1.00	.500	.500	.500	.500	.500	.500
Frontal_Med_Orb_R	0.23	<b>&lt;0.01</b>	0.77	.126	.500	.059	.439	.500	.095
Rectus_L	0.25	<b>&lt;0.01</b>	0.75	<b>.036</b>	.500	<b>.013</b>	.338	.500	<b>.033</b>
Rectus_R	0.16	<b>&lt;0.01</b>	0.84	.179	.500	.155	.451	.500	.201
Insula_L	0.40	<b>&lt;0.01</b>	0.60	<b>.003</b>	.500	<b>&lt;.001</b>	.106	.500	<b>.003</b>
Insula_R	0.52	<b>&lt;0.01</b>	0.48	<b>&lt;.001</b>	.500	<b>&lt;.001</b>	<b>.045</b>	.500	<b>&lt;.001</b>
Cingulum_Ant_L	0.23	0.08	0.70	.220	.358	<b>.004</b>	.463	.500	<b>.011</b>
Cingulum_Ant_R	<b>&lt;0.01</b>	0.19	0.81	.500	.074	<b>.020</b>	.500	.500	<b>.041</b>
Cingulum_Mid_L	0.40	<b>&lt;0.01</b>	0.60	<b>.038</b>	.500	<b>&lt;.001</b>	.338	.500	<b>.001</b>
Cingulum_Mid_R	0.02	0.22	0.76	.475	.163	<b>.003</b>	.500	.500	<b>.010</b>
Cingulum_Post_L	<b>&lt;0.01</b>	<b>&lt;0.01</b>	1.00	.487	.500	.500	.500	.500	.500
Cingulum_Post_R	<b>&lt;0.01</b>	0.12	0.88	.500	.192	.148	.500	.500	.195
ParaHippocampal_L	0.42	<b>&lt;0.01</b>	0.58	<b>.014</b>	.500	<b>&lt;.001</b>	.204	.500	<b>.003</b>
ParaHippocampal_R	0.31	<b>&lt;0.01</b>	0.69	<b>.015</b>	.500	<b>.021</b>	.204	.500	<b>.042</b>
Calcarine_L	<b>&lt;0.01</b>	0.18	0.82	.500	.147	<b>.029</b>	.500	.500	.052
Calcarine_R	0.24	<b>&lt;0.01</b>	0.76	.223	.500	<b>.043</b>	.463	.500	.074
Cuneus_L	0.07	0.07	0.85	.404	.376	.130	.500	.500	.180
Cuneus_R	<b>&lt;0.01</b>	0.13	0.87	.500	.204	.102	.500	.500	.147
Lingual_L	<b>&lt;0.01</b>	0.25	0.75	.500	.053	<b>.002</b>	.500	.500	<b>.008</b>
Lingual_R	0.05	0.25	0.71	.446	.117	<b>&lt;.001</b>	.500	.500	<b>.003</b>
Occipital_Sup_L	<b>&lt;0.01</b>	0.19	0.81	.500	.086	<b>.017</b>	.500	.500	<b>.037</b>
Occipital_Sup_R	<b>&lt;0.01</b>	0.12	0.88	.500	.211	.148	.500	.500	.195
Occipital_Mid_L	0.02	0.20	0.78	.468	.181	<b>.008</b>	.500	.500	<b>.021</b>
Occipital_Mid_R	0.06	<b>&lt;0.01</b>	0.94	.252	.500	.400	.498	.500	.439
Occipital_Inf_L	0.17	<b>&lt;0.01</b>	0.83	.146	.500	.183	.451	.500	.225
Occipital_Inf_R	0.41	<b>&lt;0.01</b>	0.59	<b>.038</b>	.500	<b>&lt;.001</b>	.338	.500	<b>.003</b>

(Continues)



TABLE 5 (Continued)

Region of interest	Variance components			Hypothesis test <i>p</i> -values			Hypothesis test <i>Q</i> -values		
	<i>a</i> <sup>2</sup>	<i>c</i> <sup>2</sup>	<i>e</i> <sup>2</sup>	A	C	A and C	A	C	A and C
Fusiform_L	0.31	<0.01	0.69	.107	.500	<b>.007</b>	.439	.500	<b>.018</b>
Fusiform_R	0.19	0.26	0.56	.242	.083	<b>&lt;.001</b>	.491	.500	<b>&lt;.001</b>
Postcentral_L	0.35	<0.01	0.65	.078	.500	<b>.002</b>	.363	.500	<b>.007</b>
Postcentral_R	0.27	<0.01	0.73	.113	.500	<b>.016</b>	.439	.500	<b>.037</b>
Parietal_Sup_L	0.02	0.27	0.71	.467	.114	<b>&lt;.001</b>	.500	.500	<b>.003</b>
Parietal_Sup_R	<0.01	0.12	0.88	.500	.050	.130	.500	.500	.180
Parietal_Inf_L	0.18	<0.01	0.82	.194	.500	.095	.463	.500	.141
Parietal_Inf_R	<0.01	0.11	0.89	.500	.286	.163	.500	.500	.207
SupraMarginal_L	0.13	<0.01	0.87	.318	.500	.256	.500	.500	.301
SupraMarginal_R	0.17	0.06	0.78	.311	.400	<b>.046</b>	.500	.500	.078
Angular_L	<0.01	<0.01	1.00	.500	.500	.500	.500	.500	.500
Angular_R	0.24	<0.01	0.76	.173	.500	<b>.025</b>	.451	.500	<b>.049</b>
Precuneus_L	0.22	<0.01	0.78	.097	.500	<b>.048</b>	.424	.500	.078
Precuneus_R	0.17	<0.01	0.83	.219	.500	.132	.463	.500	.180
Paracentral_Lobule_L	0.32	<0.01	0.68	.063	.500	<b>.002</b>	.363	.500	<b>.008</b>
Paracentral_Lobule_R	0.03	<0.01	0.97	.385	.500	.479	.500	.500	.500
Heschl_L	0.08	<0.01	0.92	.300	.500	.377	.500	.500	.426
Heschl_R	0.42	<0.01	0.58	<b>.008</b>	.500	<b>&lt;.001</b>	.202	.500	<b>.003</b>
Temporal_Sup_L	0.31	<0.01	0.69	.075	.500	<b>.008</b>	.363	.500	<b>.021</b>
Temporal_Sup_R	0.22	<0.01	0.78	.054	.500	.069	.363	.500	.109
Temporal_Pole_Sup_L	0.14	0.04	0.82	.325	.429	.087	.500	.500	.134
Temporal_Pole_Sup_R	<0.01	0.18	0.82	.500	.130	<b>.027</b>	.500	.500	<b>.050</b>
Temporal_Mid_L	0.25	<0.01	0.75	.075	.500	<b>.030</b>	.363	.500	.053
Temporal_Mid_R	0.37	<0.01	0.63	.064	.500	<b>&lt;.001</b>	.363	.500	<b>.004</b>
Temporal_Pole_Mid_L	0.06	<0.01	0.94	.274	.500	.418	.500	.500	.452
Temporal_Pole_Mid_R	0.32	<0.01	0.68	.071	.500	<b>.002</b>	.363	.500	<b>.008</b>
Temporal_Inf_L	0.35	<0.01	0.65	<b>.015</b>	.500	<b>&lt;.001</b>	.204	.500	<b>.004</b>
Temporal_Inf_R	0.26	<0.01	0.74	.179	.500	<b>.027</b>	.451	.500	.050

A = test of genetic effects; C = test of shared environmental effects; A and C = test of familial effects (genetic + environmental). Bold/italicized text indicates *p*-values (unadjusted for multiple comparisons) and *q* - values (adjusted for multiple comparisons) below 0.05.

genetic influences on total SA and significant genetic overlap between CT and SA. These findings provide a deeper understanding of CT and SA development and contribute critical insight into how genetic influences shape cortical structure across the human lifespan.

We found that genetic influences determine a significant portion of individual differences in neonatal total SA. Specifically, when controlling for important obstetric history variables, we observed a high heritability estimate of 0.78. During the early postnatal period, cortical SA expands dramatically, with 0.50% daily growth in the first month (Jha et al., 2018) and average growth of 114% in the first 2 years (Lyall et al., 2015). Genetic influences driving total SA during early development likely control the tangential expansion of the cortex by impacting symmetric divisions of ventricular radial glia during early neurogenesis and outer radial glia during late neurogenesis (Nowakowski et al., 2016; Rakic, 2009). Genes involved in the development of sulci, gyri, and cortico-cortical connectivity may also impact individual differences in total SA observed in our study (Lewitus, Kelava, & Huttner, 2013).

Interestingly, when controlling only for variables most often used in adult studies (age, sex, and scanning protocol) the heritability estimate remained significant but was greatly reduced. Compared with

adult twin and family studies, which report high estimates of 0.89 and 0.71, respectively (Panizzon et al., 2009; Winkler et al., 2010), genetic influences seem to play a significant but smaller role in explaining individual differences in total SA at birth. Moreover, while traditional adult studies report no effects of the common environment, we found that common environmental influences play a substantial role in explaining the variation observed in neonatal total SA. We note that significant influences of the common environment largely disappear when controlling for obstetric variables, suggesting that strong environmental influences are likely driven by the impacts of gestational age at birth and birth weight on neonatal brain structure. A recent study of the EBDS sample revealed that both gestational age at birth and birth weight are important predictors of neonatal total SA (Jha et al., 2018). Taken together, results from both analyses reveal that genetic influences are important determinants of neonatal SA but heritability estimates should be interpreted with caution as they may vary based on covariates.

In contrast to total SA, genetic influences did not explain a significant proportion of the variation observed in neonatal average CT. Moreover, the observed heritability in our neonatal sample (0.29)

**TABLE 6** Univariate ACE model maximum likelihood parameter estimates and *p*-values for regional SA measures

Region of interest	Variance components			Hypothesis test <i>p</i> -values			Hypothesis test <i>Q</i> -values		
	$a^2$	$c^2$	$e^2$	A	C	A and C	A	C	A and C
Precentral_L	0.27	0.10	0.63	.168	.316	<.001	.247	.500	.001
Precentral_R	0.18	0.18	0.64	.252	.196	<.001	.312	.500	<.001
Frontal_Sup_L	0.03	0.18	0.79	.466	.204	.014	.500	.500	.021
Frontal_Sup_R	0.23	0.11	0.66	.209	.300	.001	.281	.500	.002
Frontal_Sup_Orb_L	0.32	<0.01	0.68	.049	.500	.004	.137	.500	.008
Frontal_Sup_Orb_R	0.02	<0.01	0.98	.465	.500	.495	.500	.500	.500
Frontal_Mid_L	0.38	<0.01	0.62	.010	.500	.001	.065	.500	.003
Frontal_Mid_R	0.29	0.18	0.52	.119	.159	<.001	.201	.500	<.001
Frontal_Mid_Orb_L	0.23	<0.01	0.77	.115	.500	.049	.200	.500	.065
Frontal_Mid_Orb_R	0.30	<0.01	0.70	.019	.500	.008	.083	.500	.014
Frontal_Inf_Oper_L	0.08	<0.01	0.92	.316	.500	.372	.368	.500	.397
Frontal_Inf_Oper_R	0.05	<0.01	0.95	.353	.500	.466	.405	.500	.484
Frontal_Inf_Tri_L	0.11	<0.01	0.89	.244	.500	.288	.312	.500	.321
Frontal_Inf_Tri_R	0.31	<0.01	0.69	.073	.500	.008	.168	.500	.014
Frontal_Inf_Orb_L	0.56	<0.01	0.44	<.001	.500	<.001	.003	.500	<.001
Frontal_Inf_Orb_R	0.51	<0.01	0.49	.012	.500	<.001	.069	.500	<.001
Rolandic_Oper_L	0.35	<0.01	0.65	.024	.500	.002	.089	.500	.004
Rolandic_Oper_R	0.43	<0.01	0.57	.039	.500	<.001	.117	.500	.001
Supp_Motor_Area_L	0.35	0.06	0.58	.095	.374	<.001	.178	.500	<.001
Supp_Motor_Area_R	0.18	0.14	0.68	.275	.253	.001	.330	.500	.003
Olfactory_L	0.13	<0.01	0.87	.145	.500	.239	.231	.500	.270
Olfactory_R	0.28	<0.01	0.72	.023	.500	.015	.089	.500	.021
Frontal_Sup_Medial_L	0.31	<0.01	0.69	.077	.500	.011	.170	.500	.018
Frontal_Sup_Medial_R	0.08	<0.01	0.92	.249	.500	.384	.312	.500	.405
Frontal_Med_Orb_L	<0.01	0.08	0.92	.500	.310	.301	.500	.500	.326
Frontal_Med_Orb_R	0.20	0.12	0.68	.247	.275	.001	.312	.500	.003
Rectus_L	0.22	<0.01	0.78	.088	.500	.090	.176	.500	.107
Rectus_R	0.04	0.13	0.83	.447	.281	.054	.498	.500	.069
Insula_L	0.76	<0.01	0.24	<.001	.500	<.001	.001	.500	<.001
Insula_R	0.64	<0.01	0.36	<.001	.500	<.001	.005	.500	<.001
Cingulum_Ant_L	0.24	<0.01	0.76	.069	.500	.063	.168	.500	.077
Cingulum_Ant_R	0.33	<0.01	0.67	.020	.500	.013	.083	.500	.020
Cingulum_Mid_L	0.32	<0.01	0.68	.096	.500	.009	.178	.500	.015
Cingulum_Mid_R	0.37	<0.01	0.63	.017	.500	.003	.083	.500	.006
Cingulum_Post_L	0.29	<0.01	0.71	.032	.500	.018	.104	.500	.026
Cingulum_Post_R	0.11	<0.01	0.88	.374	.495	.294	.423	.500	.324
ParaHippocampal_L	0.18	<0.01	0.82	.080	.500	.128	.173	.500	.147
ParaHippocampal_R	0.30	0.11	0.59	.148	.285	<.001	.231	.500	<.001
Calcarine_L	0.28	0.24	0.48	.110	.090	<.001	.195	.500	<.001
Calcarine_R	0.49	<0.01	0.51	.029	.500	<.001	.098	.500	<.001
Cuneus_L	0.18	0.03	0.79	.280	.446	.056	.331	.500	.070
Cuneus_R	0.26	<0.01	0.74	.058	.500	.037	.152	.500	.050
Lingual_L	0.54	<0.01	0.46	.019	.489	<.001	.083	.500	<.001
Lingual_R	0.21	0.34	0.46	.166	.027	<.001	.247	.500	<.001
Occipital_Sup_L	0.45	<0.01	0.55	.006	.500	<.001	.057	.500	<.001
Occipital_Sup_R	0.47	<0.01	0.53	.019	.500	<.001	.083	.500	<.001
Occipital_Mid_L	0.50	<0.01	0.50	.007	.500	<.001	.057	.500	<.001
Occipital_Mid_R	<0.01	0.24	0.76	.500	.103	.002	.500	.500	.005
Occipital_Inf_L	<0.01	0.14	0.86	.500	.257	.098	.500	.500	.114
Occipital_Inf_R	0.23	<0.01	0.77	.175	.500	.033	.252	.500	.046

(Continues)

TABLE 6 (Continued)

Region of interest	Variance components			Hypothesis test <i>p</i> -values			Hypothesis test <i>Q</i> -values		
	<i>a</i> <sup>2</sup>	<i>c</i> <sup>2</sup>	<i>e</i> <sup>2</sup>	A	C	A and C	A	C	A and C
Fusiform_L	0.29	0.05	0.66	.145	.414	<b>.001</b>	.231	.500	<b>.001</b>
Fusiform_R	0.26	<0.01	0.74	.154	.500	<b>.018</b>	.236	.500	<b>.026</b>
Postcentral_L	0.36	<0.01	0.64	.053	.500	<b>&lt;.001</b>	.142	.500	<b>.001</b>
Postcentral_R	0.35	<0.01	0.65	.069	.500	<b>.003</b>	.168	.500	<b>.006</b>
Parietal_Sup_L	<0.01	<0.01	1.00	.500	.500	.500	.500	.500	.500
Parietal_Sup_R	0.50	0.03	0.47	<b>.029</b>	.430	<b>&lt;.001</b>	.098	.500	<b>&lt;.001</b>
Parietal_Inf_L	0.02	0.29	0.69	.480	.073	<b>&lt;.001</b>	.500	.500	<b>&lt;.001</b>
Parietal_Inf_R	0.19	0.07	0.74	.256	.376	<b>.008</b>	.312	.500	<b>.014</b>
SupraMarginal_L	<0.01	<0.01	1.00	.500	.500	.500	.500	.500	.500
SupraMarginal_R	0.40	<0.01	0.60	<b>.003</b>	.500	<b>&lt;.001</b>	<b>.041</b>	.500	<b>.001</b>
Angular_L	0.21	<0.01	0.79	.072	.500	.064	.168	.500	.077
Angular_R	0.22	0.08	0.70	.212	.357	<b>.001</b>	.281	.500	<b>.003</b>
Precuneus_L	0.58	<0.01	0.42	<b>&lt;.001</b>	.500	<b>&lt;.001</b>	<b>.006</b>	.500	<b>&lt;.001</b>
Precuneus_R	0.63	<0.01	0.37	<b>.001</b>	.500	<b>&lt;.001</b>	<b>.008</b>	.500	<b>&lt;.001</b>
Paracentral_Lobule_L	0.43	<0.01	0.57	<b>.012</b>	.500	<b>.001</b>	.069	.500	<b>.003</b>
Paracentral_Lobule_R	0.32	<0.01	0.68	<b>.046</b>	.500	<b>.003</b>	.134	.500	<b>.006</b>
Heschl_L	0.39	<0.01	0.61	<b>.007</b>	.500	<b>.002</b>	.057	.500	<b>.005</b>
Heschl_R	0.21	<0.01	0.79	.107	.500	.051	.194	.500	.066
Temporal_Sup_L	0.39	0.04	0.57	.085	.426	<b>&lt;.001</b>	.176	.500	<b>&lt;.001</b>
Temporal_Sup_R	0.44	<0.01	0.56	<b>.039</b>	.500	<b>&lt;.001</b>	.117	.500	<b>&lt;.001</b>
Temporal_Pole_Sup_L	0.23	0.10	0.67	.206	.314	<b>.001</b>	.281	.500	<b>.002</b>
Temporal_Pole_Sup_R	0.26	0.04	0.70	.184	.423	<b>.003</b>	.256	.500	<b>.006</b>
Temporal_Mid_L	0.34	<0.01	0.66	<b>.008</b>	.500	<b>.003</b>	.059	.500	<b>.006</b>
Temporal_Mid_R	0.31	<0.01	0.69	.132	.500	<b>.011</b>	.218	.500	<b>.017</b>
Temporal_Pole_Mid_L	0.24	0.13	0.63	.184	.275	<b>&lt;.001</b>	.256	.500	<b>&lt;.001</b>
Temporal_Pole_Mid_R	0.22	<0.01	0.78	.090	.500	.055	.176	.500	.069
Temporal_Inf_L	0.24	<0.01	0.76	.088	.500	<b>.045</b>	.176	.500	.061
Temporal_Inf_R	0.58	<0.01	0.42	<b>.004</b>	.500	<b>&lt;.001</b>	<b>.048</b>	.500	<b>&lt;.001</b>

A = test of genetic effects; C = test of shared environmental effects; A and C = test of familial effects (genetic + environmental). Bold/italicized text indicates *p*-values (unadjusted for multiple comparisons) and *q* - values (adjusted for multiple comparisons) below 0.05.

was smaller compared with heritability estimates (0.81 and 0.69) reported in adults (Panizzon et al., 2009; Winkler et al., 2010). Imaging studies have revealed significant growth in CT in the neonatal period (Jha et al., 2018; Lyall et al., 2015) and continuing in the first year of life (Remer et al., 2017). Rapid thickening of the cortex peaks during this period and is followed by gradual linear decreases throughout childhood, adolescence, and adulthood (Ducharme et al., 2016; Wierenga, Langen, Oranje, & Durston, 2014). We note that for CT, myelination of the underlying WM may be of particular importance as it affects tissue contrast at the WM/GM boundary. This may have important implications in terms of image processing (Walhovd, Fjell, Giedd, Dale, & Brown, 2017) and heritability outcomes. Additionally, adolescent and adult twin studies reveal significant genetic correlations between GM thickness and white matter connectivity (Kochunov et al., 2011; Shen et al., 2016) suggesting that heritability of neonatal CT may be related to genes driving neonatal WM.

In general, our findings suggest that genetic influences on average CT and total SA may increase between the neonatal period and adulthood. In adults, individual differences in average CT and total SA may be related to genes impacting the number and size of neurons, glia,

and synaptic machinery (De Graaf-Peters & Hadders-Algra, 2006; Rakic, 2009) and pathways controlling processes of synaptic pruning, myelination, and aging (Stiles & Jernigan, 2010). A potential increase in heritability for total SA and average CT between neonates and adults could also be interpreted as canalization (Gilmore et al., 2010; Lenroot & Giedd, 2008), the concept that heritability of a phenotype will increase as various genetic influences act over development under expected environmental conditions. To best understand how early postnatal genetic influences compare to genetic influences during later ages, heritability studies of total SA and average CT should be performed during late infancy, childhood, and early adolescence.

Our most remarkable and unexpected finding regarding total SA and average CT was the strong genetic overlap between these global measures. We found that the shared genetic effect between neonatal CT and total SA is high ( $r_G = 0.65$ ). Thus far, studies comparing CT and SA in adults have found little to no genetic associations between the two phenotypes (Panizzon et al., 2009; Winkler et al., 2010). Based on such reports, it has been suggested that CT and SA are driven by two distinct sets of genetic influences related to distinct developmental events during early prenatal life. In contrast to these

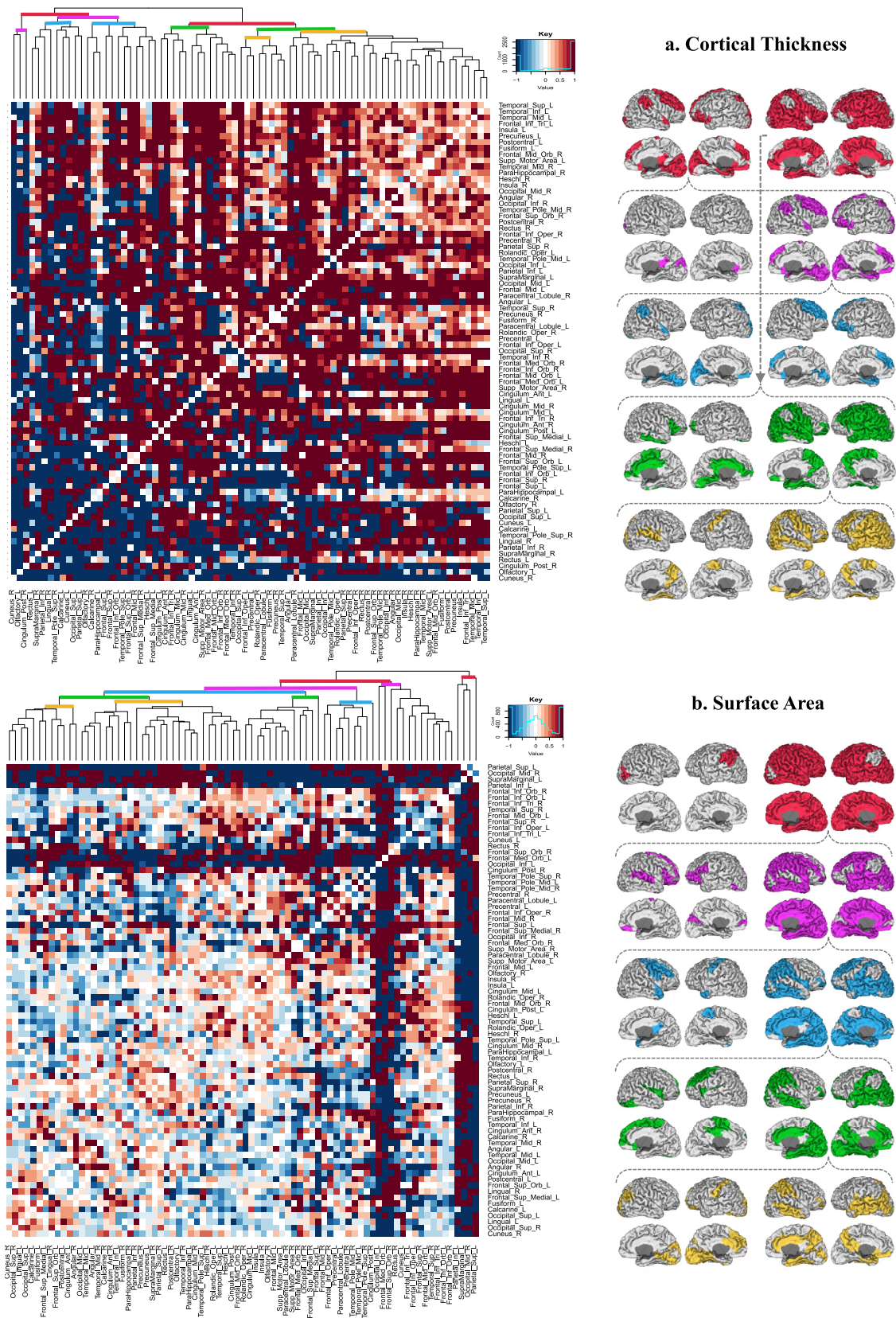


**FIGURE 2** Heatmap of genetic correlations between 78 ROIs of (a) neonatal cortical thickness and (b) neonatal surface area. Dendrograms are displayed on each heatmap to present the results from a hierachal cluster analysis. Clusters are visually displayed on the neonatal brain surface



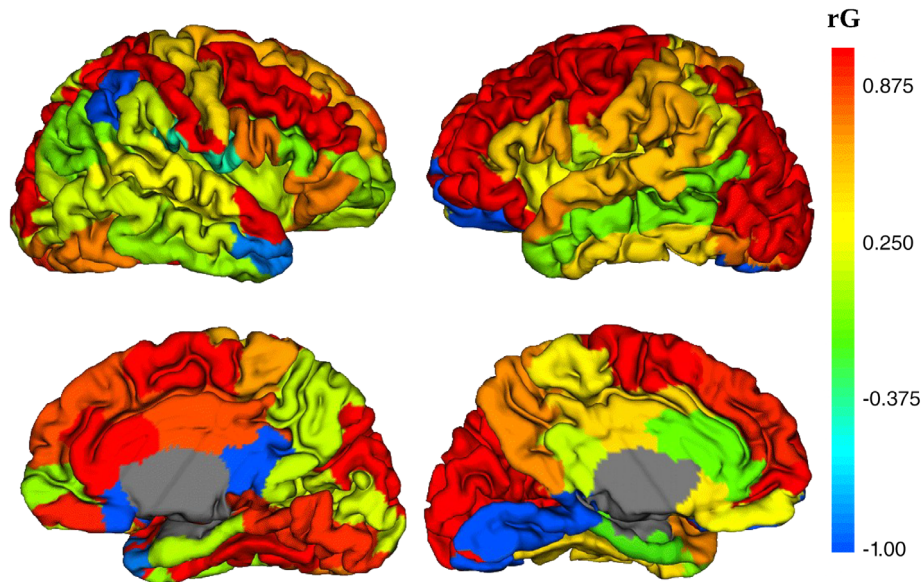


**FIGURE 3** Genetic correlations (rG) between neonatal cortical thickness and surface area for each ROI projected onto the cortical surface. Subcortical regions are in gray and were not analyzed

findings, our twin neonate study reveals that early genetic influences on CT and SA are actually similar and overlapping. The association we observe between total SA and average CT is likely reflective of broad-ranging genetic influences that control general molecular mechanisms involved in cortical development and those which coordinate the tangential and radial expansion during the fetal and early postnatal periods (Silbereis et al., 2016). In fact, developmental studies in

rodents reveal that many genes involved in cortical patterning or the proliferation of founder cells also play a role in determining the thickness of the cortex by controlling neuron number and size (Georgala, Manuel, & Price, 2011; Korada, Zheng, Basilio, Schwartz, & Vaccarino, 2002). Genetic overlap between CT and SA is also evident regionally across the neonatal cortex, with about 60% of ROIs showing genetic correlations of 0.3 or above. Our assessment of neonatal CT

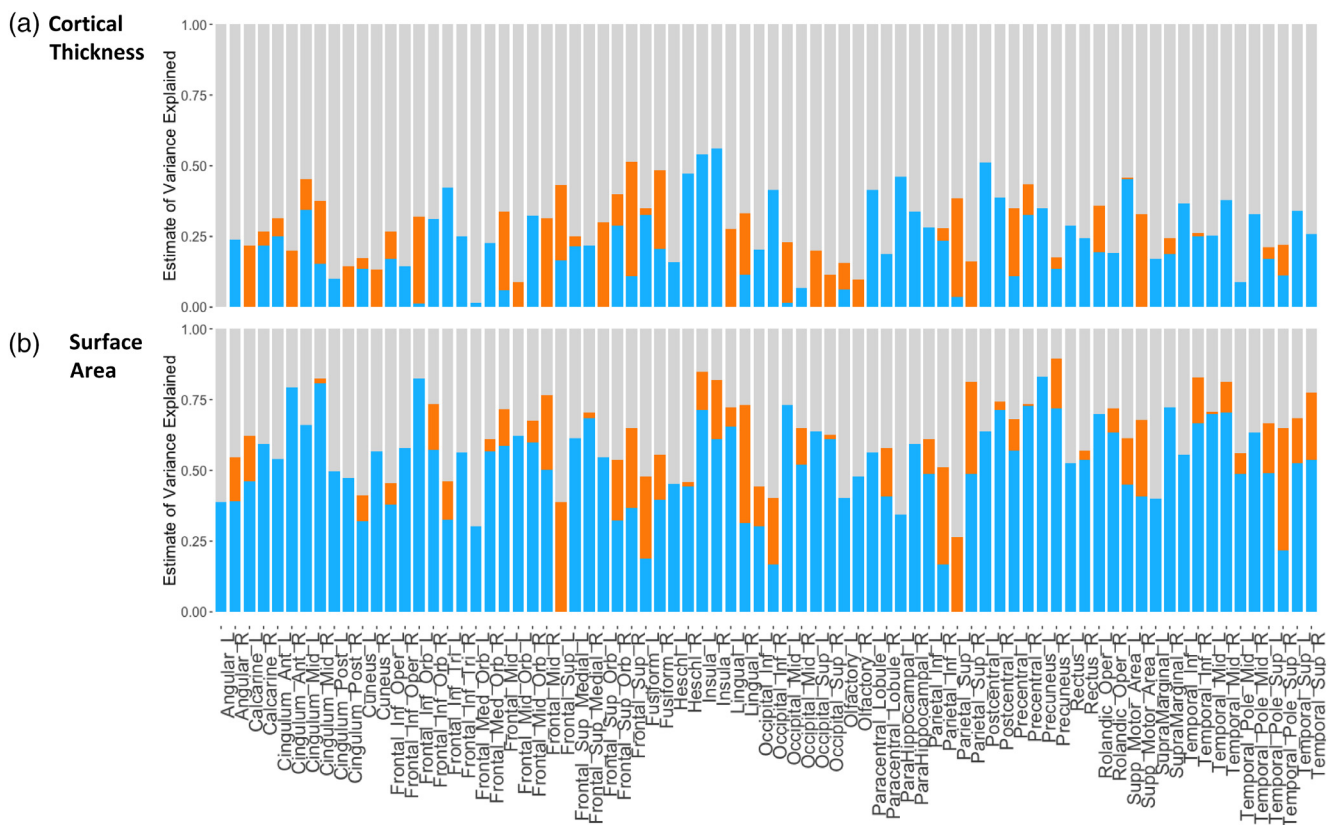


**FIGURE 4** Genetic, common environmental, and unique environmental influences for regional neonatal (a) cortical thickness and (b) surface area without adjustments for global brain measures. Genetic influences are displayed in blue, common environmental influences are displayed in orange, and unique environmental influences are displayed in gray



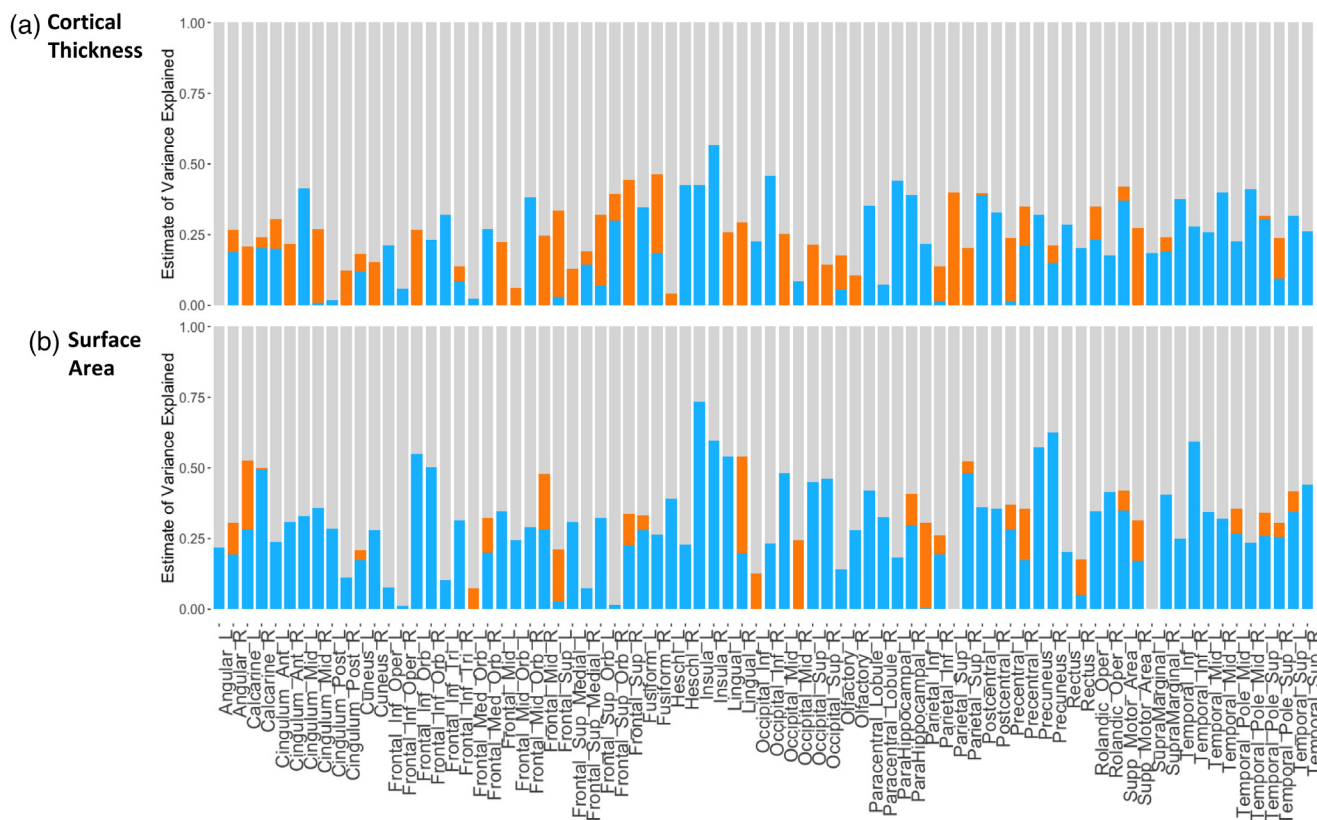


**FIGURE 5** Genetic, common environmental, and unique environmental influences for regional neonatal (a) cortical thickness and (b) surface area with adjustments for brain size, age, sex, and scanner parameters. Genetic influences are displayed in blue, common environmental influences are displayed in orange, and unique environmental influences are displayed in gray

and SA serves as the earliest reported snapshot of genetic effects on brain structure and provides evidence of a dynamic genetic relationship between these two features across different periods of development. Additionally, findings suggest that differences in CT and SA observed in adult studies may not be reflective of fetal differences in radial and tangential expansion of the cortex but rather may be influenced by cellular and genetic processes implicated in myelination, synaptic pruning, or neuronal degeneration. To better understand the genetic relationship between CT and SA during the prenatal period, comparable fetal MRI studies of global cortical structure are critical. Moreover, longitudinal studies of global cortical structure from infancy to adulthood will provide insight into the genetic association of CT and SA across the lifespan.

At the regional level, genetic influences accounted for <1 to 76% of variation in SA and <1% to 52% of the variation in CT across the cortex. In adult samples, Panizzon et al. (2009) found genetic influences ranging from 3 to 74% for regional SA and from 20 to 76% for regional CT and Winkler et al. (2010) found genetic influences ranging from 17 to 76% regional SA and from 6 to 73% for regional CT. When comparing our findings to these studies, we note that genetic influences during infancy explain a smaller percent of the total phenotypic variation in CT and SA. Moreover, while we observe considerable heterogeneity in regional heritability estimates, genetic influences remain largely nonsignificant in our sample. The exceptions are the heritability estimates for SA in the insular cortex and precuneus, which are similar to those found in adults and in the right supramarginal, right inferior temporal, and left inferior orbitofrontal gyri.

Furthermore, when examining heritability estimates across all 78 ROIs, we did not observe clear regional patterns based on structural, functional, or maturational organization. Nor did we observe meaningful patterns of regionalization when examining the genetic correlations among regions of CT and SA. Together, these results suggest that individual differences in CT and SA are likely driven by a common set of underlying genetic factors influencing cortical structure at the global level. This is in contrast to twin studies of regional CT in older populations which reveal that regional heritability estimates align with maturational patterns. Specifically, in early childhood, CT in primary sensory and motor regions is highly heritable and at older ages, heritability is higher in dorsal prefrontal and temporal lobes (Lenroot et al., 2009). Moreover, twin studies of genetic regionalization in older adults have found up to 12 genetically similar clusters. Genetic divisions of SA follow an anterior–posterior division with spatially contiguous regions being genetically correlated. Genetic divisions of CT follow a basic dorsal–ventral pattern and are driven by similarities of maturational timing (Chen et al., 2011, 2012, 2013).

While our cluster analysis suggests that there are groupings of genetic covariance across the neonatal brain, these groupings do not have obvious biological correlates. For primary CT, genetic clusters are visible in the right frontal lobe, bilateral medial occipital lobe, and bilateral cingulate gyrus. For primary SA, genetic clustering is observed within the temporal lobe and precuneus as well as the medial occipital lobe. Overall however, gradients of gene expression driving cortical arealization during adulthood do not seem to contribute to clear anterior–posterior or dorsal–ventral distinctions across the neonatal

cortex. Additionally, while we observed both positive and negative genetic correlations, neither type clustered together in an exclusive manner when hierarchical clustering analyses were performed. Instead, both negative and positive genetic correlations were observed across and within all regions of the cortex. The general lack of significant regional genetic patterns in our sample is in keeping with studies of cortical gene expression which suggest that there are minimal interareal differences in gene expression across the cortex during infancy (Kang et al., 2011; Pletikos et al., 2014; Silbereis et al., 2016). This period is characterized by general neuronal and glial proliferation transcriptional programs (Pletikos et al., 2014) that are involved in the construction and maturation of neuronal circuitry and are sensitive to experience and external inputs from the environment. Significant regional differences in genetic studies of CT and SA observed in studies of older populations are likely reflections of increasing interareal differences across the cortex during adolescence and adulthood (Pletikos et al., 2014).

By performing the first twin study of infant CT and SA, we show genetics are important determinants of individual differences in neonatal cortical structure. Our findings provide important data points previously unavailable for the understanding of genetic contributions to CT and SA across the lifespan. Strengths of this study include a unique sample, extensive demographic data, and the application of cutting-edge infant image analysis methods. Limitations of this study are largely centered on the challenges of infant neuroimaging. While offering many unprecedented opportunities to study neurodevelopment, our pediatric population may be underpowered to detect significant shared environmental effects. Additionally, our use of predefined cortical regions may limit our ability to find genetic relationships across regions of the cortex, if those relationships do not adhere to classic anatomical boundaries. However, it should be noted that cortical parcellations based on genetic data do reveal genetic divisions that largely correspond to anatomical divisions similar to those used in the current study (Chen et al., 2012). Future studies should focus on pursuing a non-biased approach of using vertex-based analysis to generate continuous maps of genetic influences on CT and SA. Moreover, results from our analysis are based on one infant dataset and may not be generalizable to other pediatric populations. However, because there are no genetic investigations of CT or SA in young typically developing infants, results from this study are highly informative. Findings provide cortical regions to prioritize for future imaging genetic studies and valuable targets to better understand genetic processes that contribute to psychiatric and developmental disorders.

## ACKNOWLEDGMENTS

This work was supported by the National Institutes of Health (MH064065, MH070890, and HD053000 to JG, MH083045 to RK, UL1 RR025747, and MH086633 to HZ, MH091645, HD-003110 and HD079124 to MS, MH108914 and MH107815 to GL, MH100217 to DS, MH109773 to LW, T32 NS007431 to SJ, JB, and VM, K01ES026840 to ES, and R25GM055336 to VM), and the National Science Foundation (SES-1357666 and DMS-1407655 to HZ). We thank our participating families and staff of the UNC MRI Research Center, the UNC Neuro Image Research and Analysis Laboratories, Brain & Behavior Research Foundation, the John and Polly Sparks Foundation and the UNC Early Brain Development Study. No conflicts of interest are reported.

## ORCID

Jessica B. Girault  <https://orcid.org/0000-0002-9271-0354>

Li Wang  <https://orcid.org/0000-0003-2165-0080>

John H. Gilmore  <https://orcid.org/0000-0002-0939-6764>

## REFERENCES

- Benjamini, Y., & Hochberg, Y. (2000). On the adaptive control of the false discovery rate in multiple testing with independent statistics. *Journal of Educational and Behavioral Statistics*, 25, 60–83.
- Boker, S., Neale, M., Maes, H., Wilde, M., Spiegel, M., Brick, T., ... Fox, J. (2011). OpenMx: An open source extended structural equation modeling framework. *Psychometrika*, 76, 306–317.
- Budday, S., Steinmann, P., & Kuhl, E. (2015). Physical biology of human brain development. *Frontiers in Cellular Neuroscience*, 9, 257.
- Chen, C.-H., Fiecas, M., Gutiérrez, E. D., Panizzon, M. S., Eyer, L. T., Vuoksimaa, E., ... Kremen, W. S. (2013). Genetic topography of brain morphology. *Proceedings of the National Academy of Sciences of the United States of America*, 110, 17089–17094.
- Chen, C.-H., Gutiérrez, E. D., Thompson, W., Panizzon, M. S., Jernigan, T. L., Eyer, L. T., ... Dale, A. M. (2012). Hierarchical genetic organization of human cortical surface area. *Science*, 335, 1634–1636.
- Chen, C.-H., Panizzon, M. S., Eyer, L. T., Jernigan, T. L., Thompson, W., Fennema-Notestine, C., ... Dale, A. M. (2011). Genetic influences on cortical regionalization in the human brain. *Neuron*, 72, 537–544.
- De Graaf-Peters, V. B., & Hadders-Algra, M. (2006). Ontogeny of the human central nervous system: What is happening when? *Early Human Development*, 82, 257–266.
- Dominicus, A., Skrondal, A., Gjessing, H. K., Pedersen, N. L., & Palmgren, J. (2006). Likelihood ratio tests in behavioral genetics: Problems and solutions. *Behavior Genetics*, 36, 331–340.
- Dubois, J., Dehaene-Lambertz, G., Kulikova, S., Poupon, C., Hüppi, P. S., & Hertz-Pannier, L. (2014). The early development of brain white matter: A review of imaging studies in fetuses, newborns and infants. *Neuroscience*, 276, 48–71.
- Ducharme, S., Albaugh, M. D., Nguyen, T.-V., Hudziak, J. J., Mateos-Pérez, J. M., Labbe, A., ... Brain Development Cooperative Group. (2016). Trajectories of cortical thickness maturation in normal brain development—the importance of quality control procedures. *NeuroImage*, 125, 267–279.
- Fischl, B., Sereno, M. I., & Dale, A. M. (1999). Cortical surface-based analysis. II: Inflation, flattening, and a surface-based coordinate system. *NeuroImage*, 9, 195–207.
- Georgala, P. A., Manuel, M., & Price, D. J. (2011). The generation of superficial cortical layers is regulated by levels of the transcription factor Pax6. *Cerebral Cortex*, 21, 81–94.
- Gilmore, J. H., Knickmeyer, R. C., & Gao, W. (2018). Imaging structural and functional brain development in early childhood. *Nature Reviews. Neuroscience*, 19, 123–137.
- Gilmore, J. H., Schmitt, J. E., Knickmeyer, R. C., Smith, J. K., Lin, W., Styner, M., ... Neale, M. C. (2010). Genetic and environmental contributions to neonatal brain structure: A twin study. *Human Brain Mapping*, 31, 1174–1182.
- Gilmore, J. H., Shi, F., Woolson, S. L., Knickmeyer, R. C., Short, S. J., Lin, W., ... Shen, D. (2012). Longitudinal development of cortical and subcortical gray matter from birth to 2 years. *Cerebral Cortex*, 22, 2478–2485.
- Hill, J., Dierker, D., Neil, J., Inder, T., Knutsen, A., Harwell, J., ... Van Essen, D. (2010). A surface-based analysis of hemispheric asymmetries and folding of cerebral cortex in term-born human infants. *The Journal of Neuroscience*, 30, 2268–2276.
- Janssen, J., Alemán-Gómez, Y., Schnack, H., Balaban, E., Pina-Camacho, L., Alfaro-Almagro, F., ... Desco, M. (2014). Cortical morphology of adolescents with bipolar disorder and with schizophrenia. *Schizophrenia Research*, 158, 91–99.
- Jha, S. C., Xia, K., Ahn, M., Girault, J. B., Li, G., Wang, L., ... Knickmeyer, R. C. (2018). Environmental influences on infant cortical thickness and surface area. *Cerebral Cortex*, 22, 1539.

- Kang, H. J., Kawasawa, Y. I., Cheng, F., Zhu, Y., Xu, X., Li, M., ... Sestan, N. (2011). Spatio-temporal transcriptome of the human brain. *Nature*, *478*, 483–489.
- Knickmeyer, R. C., Gouttard, S., Kang, C., Evans, D., Wilber, K., Smith, J. K., ... Gilmore, J. H. (2008). A structural MRI study of human brain development from birth to 2 years. *The Journal of Neuroscience*, *28*, 12176–12182.
- Knickmeyer, R. C., Xia, K., Lu, Z., Ahn, M., Jha, S. C., Zou, F., ... Gilmore, J. H. (2016). Impact of demographic and obstetric factors on infant brain volumes: A population neuroscience study. *Cerebral Cortex*, *27*(12), 5616–5625.
- Kochunov, P., Castro, C., Davis, D., Dudley, D., Brewer, J., Zhang, Y., ... Schatten, G. (2010). Mapping primary gyrogenesis during fetal development in primate brains: High-resolution in utero structural MRI of fetal brain development in pregnant baboons. *Frontiers in Neuroscience*, *4*, 20.
- Kochunov, P., Glahn, D. C., Nichols, T. E., Winkler, A. M., Hong, E. L., Holcomb, H. H., ... Blangero, J. (2011). Genetic analysis of cortical thickness and fractional anisotropy of water diffusion in the brain. *Frontiers in Neuroscience*, *5*, 120.
- Korada, S., Zheng, W., Basilico, C., Schwartz, M. L., & Vaccarino, F. M. (2002). Fibroblast growth factor 2 is necessary for the growth of glutamate projection neurons in the anterior neocortex. *The Journal of Neuroscience*, *22*, 863–875.
- Lenroot, R. K., & Giedd, J. N. (2008). The changing impact of genes and environment on brain development during childhood and adolescence: Initial findings from a neuroimaging study of pediatric twins. *Development and Psychopathology*, *20*, 1161–1175.
- Lenroot, R. K., Schmitt, J. E., Ordaz, S. J., Wallace, G. L., Neale, M. C., Lerch, J. P., ... Giedd, J. N. (2009). Differences in genetic and environmental influences on the human cerebral cortex associated with development during childhood and adolescence. *Human Brain Mapping*, *30*, 163–174.
- Lewitus, E., Kelava, I., & Huttner, W. B. (2013). Conical expansion of the outer subventricular zone and the role of neocortical folding in evolution and development. *Frontiers in Human Neuroscience*, *7*, 424.
- Li, G., Nie, J., Wang, L., Shi, F., Gilmore, J. H., Lin, W., & Shen, D. (2014). Measuring the dynamic longitudinal cortex development in infants by reconstruction of temporally consistent cortical surfaces. *NeuroImage*, *90*, 266–279.
- Li, G., Nie, J., Wang, L., Shi, F., Lin, W., Gilmore, J. H., & Shen, D. (2013). Mapping region-specific longitudinal cortical surface expansion from birth to 2 years of age. *Cerebral Cortex*, *23*, 2724–2733.
- Li, G., Nie, J., Wu, G., Wang, Y., Shen, D., & Alzheimer's Disease Neuroimaging Initiative. (2012). Consistent reconstruction of cortical surfaces from longitudinal brain MR images. *NeuroImage*, *59*, 3805–3820.
- Li, G., Wang, L., Shi, F., Lyall, A. E., Ahn, M., Peng, Z., ... Shen, D. (2016). Cortical thickness and surface area in neonates at high risk for schizophrenia. *Brain Structure & Function*, *221*, 447–461.
- Long, X., Liao, W., Jiang, C., Liang, D., Qiu, B., & Zhang, L. (2012). Healthy aging: An automatic analysis of global and regional morphological alterations of human brain. *Academic Radiology*, *19*, 785–793.
- Lyall, A. E., Shi, F., Geng, X., Woolson, S., Li, G., Wang, L., ... Gilmore, J. H. (2015). Dynamic development of regional cortical thickness and surface area in early childhood. *Cerebral Cortex*, *25*, 2204–2212.
- Neale, M., & Cardon, L. (1992). *Methodology for genetic studies of twins and families*. New York, NY: Springer Science & Business Media.
- Nowakowski, T. J., Pollen, A. A., Sandoval-Espinosa, C., & Kriegstein, A. R. (2016). Transformation of the radial glia scaffold demarcates two stages of human cerebral cortex development. *Neuron*, *91*, 1219–1227.
- Panizzon, M. S., Fennema-Notestine, C., Eyler, L. T., Jernigan, T. L., Prom-Wormley, E., Neale, M., ... Kremen, W. S. (2009). Distinct genetic influences on cortical surface area and cortical thickness. *Cerebral Cortex*, *19*, 2728–2735.
- Pletikos, M., Sousa, A. M. M., Sedmak, G., Meyer, K. A., Zhu, Y., Cheng, F., ... Sestan, N. (2014). Temporal specification and bilaterality of human neocortical topographic gene expression. *Neuron*, *81*, 321–332.
- Purcell, S. (2002). Variance components models for gene-environment interaction in twin analysis. *Twin Research*, *5*, 554–571.
- Rakic, P. (1995). A small step for the cell, a giant leap for mankind: A hypothesis of neocortical expansion during evolution. *Trends in Neurosciences*, *18*, 383–388.
- Rakic, P. (2009). Evolution of the neocortex: A perspective from developmental biology. *Nature Reviews. Neuroscience*, *10*, 724–735.
- Raznahan, A., Shaw, P., Lalonde, F., Stockman, M., Wallace, G. L., Greenstein, D., ... Giedd, J. N. (2011). How does your cortex grow? *The Journal of Neuroscience*, *31*, 7174–7177.
- Remer, J., Croteau-Chonka, E., Dean, D. C., D'Arpino, S., Dirks, H., Whitley, D., & Deoni, S. C. L. (2017). Quantifying cortical development in typically developing toddlers and young children, 1-6 years of age. *NeuroImage*, *153*, 246–261.
- Schmitt, J. E., Lenroot, R. K., Wallace, G. L., Ordaz, S., Taylor, K. N., Kabani, N., ... Giedd, J. N. (2008). Identification of genetically mediated cortical networks: A multivariate study of pediatric twins and siblings. *Cerebral Cortex*, *18*, 1737–1747.
- Shaw, P., Greenstein, D., Lerch, J., Clasen, L., Lenroot, R., Gogtay, N., ... Giedd, J. (2006). Intellectual ability and cortical development in children and adolescents. *Nature*, *440*, 676–679.
- Shen, K. K., Doré, V., Rose, S., Fripp, J., McMahon, K. L., de Zubicaray, G. I., ... Salvado, O. (2016). Heritability and genetic correlation between the cerebral cortex and associated white matter connections. *Human Brain Mapping*, *37*, 2331–2347.
- Shi, F., Yap, P.-T., Wu, G., Jia, H., Gilmore, J. H., Lin, W., & Shen, D. (2011). Infant brain atlases from neonates to 1- and 2-year-olds. (Ed. Hitoshi Okazawa). *PLoS One* *6*:e18746.
- Silbereis, J. C., Pochareddy, S., Zhu, Y., Li, M., & Sestan, N. (2016). The cellular and molecular landscapes of the developing human central nervous system. *Neuron*, *89*, 248–268.
- Stiles, J., & Jernigan, T. L. (2010). The basics of brain development. *Neuropsychology Review*, *20*, 327–348.
- Tzourio-Mazoyer, N., Landeau, B., Papathanassiou, D., Crivello, F., Etard, O., Delcroix, N., ... Joliot, M. (2002). Automated anatomical labeling of activations in SPM using a macroscopic anatomical parcellation of the MNI MRI single-subject brain. *NeuroImage*, *15*, 273–289.
- Walhovd, K. B., Fjell, A. M., Giedd, J., Dale, A. M., & Brown, T. T. (2017). Through thick and thin: A need to reconcile contradictory results on trajectories in human cortical development. *Cerebral Cortex*, *27*, 1472–1481.
- Wallace, G. L., Eric Schmitt, J., Lenroot, R., Viding, E., Ordaz, S., Rosenthal, M. A., ... Giedd, J. N. (2006). A pediatric twin study of brain morphometry. *Journal of Child Psychology and Psychiatry*, *47*, 987–993.
- Wang, L., Shi, F., Li, G., Gao, Y., Lin, W., Gilmore, J. H., & Shen, D. (2014). Segmentation of neonatal brain MR images using patch-driven level sets. *NeuroImage*, *84*, 141–158.
- Wierenga, L. M., Langen, M., Oranje, B., & Durston, S. (2014). Unique developmental trajectories of cortical thickness and surface area. *NeuroImage*, *87*, 120–126.
- Winkler, A. M., Kochunov, P., Blangero, J., Almasy, L., Zilles, K., Fox, P. T., ... Glahn, D. C. (2010). Cortical thickness or grey matter volume? The importance of selecting the phenotype for imaging genetics studies. *NeuroImage*, *53*, 1135–1146.
- Wolosin, S. M., Richardson, M. E., Hennessey, J. G., Denckla, M. B., & Mostofsky, S. H. (2009). Abnormal cerebral cortex structure in children with ADHD. *Human Brain Mapping*, *30*, 175–184.
- Xia, K., Zhang, J., Ahn, M., Jha, S., Crowley, J. J., Szatkiewicz, J., ... Knickmeyer, R. C. (2017). Genome-wide association analysis identifies common variants influencing infant brain volumes. *Translational Psychiatry*, *7*, e1188.

## SUPPORTING INFORMATION

Additional supporting information may be found online in the Supporting Information section at the end of the article.

**How to cite this article:** Jha SC, Xia K, Schmitt JE, et al. Genetic influences on neonatal cortical thickness and surface area. *Hum Brain Mapp*. 2018;39:4998–5013. <https://doi.org/10.1002/hbm.24340>